STATISTICS, OPTIMIZATION AND INFORMATION COMPUTING
Stat., Optim. Inf. Comput., Vol. **15**, June 2026, pp 4993–5011.
Published online in International Academic Press (www.IAPress.org)

Enhancing Distribution Network Performance through Optimal PV and D-STATCOM Placement and Sizing Using the Newton-Metaheuristic Optimizer

Oscar Danilo Montoya [1], Rubén Iván Bolaños [2], Luis Fernando Grisales-Noreña [3]

[1]*Facultad de Ingeniería, Universidad Distrital Francisco José de Caldas, Bogotá D.C. 110121, Colombia*
[2]*Programa de Ingeniería Eléctrica, Universidad de Pamplona, Pamplona, 760042, Colombia*
[3]*Grupo de Investigación en Alta Tensión-GRALTA, Universidad del Valle, Cali 760015, Colombia*

Abstract The high penetration of renewable energy sources in distribution networks necessitates advanced planning tools for the optimal integration of compensation technologies. While the combined siting and sizing of photovoltaic (PV) systems and distribution static compensators (D-STATCOMs) is an established strategy for losses reduction and cost minimization, existing solution methodologies often struggle to balance solution accuracy with the computational burden. This paper introduces a novel application of the Newton-Metaheuristic algorithm (NMA) to address this mixed-integer nonlinear programming (MINLP) problem. The NMA's primary novelty lies in its unique hybridization of classical numerical methods with exploratory metaheuristic principles, designed to efficiently navigate the complex discrete-continuous search space of device locations and capacities. The objective is to minimize total annualized costs—covering energy procurement, investment, and operation/maintenance—subject to AC power flow constraints. A master-slave hierarchical framework is thus proposed, wherein the NMA (master) guides the search and a successive approximations power flow solver (slave) ensures technical feasibility. Validated on standard 33- and 69-bus radial systems, the NMA achieves the lowest total costs (USD 2,290,259.24 and USD 2,395,022.55), yielding a reduction of approximately 35.55% compared to a base case without distributed resources. Furthermore, the NMA demonstrates superior computational efficiency, with execution times 4.8–17.1% faster than those of established metaheuristics like the vortex search, sine-cosine, and atan-sinc optimization algorithms. The results position the NMA as a robust, efficient, and economically effective tool, offering a superior balance between solution quality and speed for a practical planning of distribution systems with integrated renewable sources.

Keywords Newton-Metaheuristic optimizer; solar power generation; distribution static compensator; master-slave optimization approach; active and reactive power compensation

AMS 2010 subject classifications 46N10

DOI:10.19139/soic-2310-5070-3414

1. Introduction

The imperative to enhance energy efficiency in electrical networks has become central to modern power systems research, driven by global sustainability goals and the need for resilient infrastructure [1]. Distribution systems, responsible for a substantial portion of total energy losses, present a critical opportunity for optimization to meet the rising electricity demand, particularly in urban environments [2, 3]. Effective losses reduction through network optimization directly supports both reliability goals and environmental targets.

*Correspondence to: O. D. Montoya (Email: odmontoyag@udistrital.edu.co). Facultad de Ingeniería, Universidad Distrital Francisco José de Caldas, Bogotá D.C. 110121, Colombia.

ISSN 2310-5070 (online) ISSN 2311-004X (print)

Grid-connected photovoltaic systems (PVs) have emerged as key enablers of sustainable distribution networks, reducing fossil fuel dependence and greenhouse gas emissions [4, 5]. However, the inherent intermittency of solar generation poses challenges to voltage regulation and power quality [6]. To address these limitations, distribution static compensators (D-STATCOMs) are being increasingly deployed alongside PV installations, providing reactive power support that enhances voltage stability and reduces line losses [7]. This coordinated approach enables simultaneous active power injection and reactive compensation, maximizing the technical benefits of distributed generation while promoting cleaner electricity delivery [8, 9].

The simultaneous optimization of PV and D-STATCOM placement and sizing remains a complex research challenge due to the nonlinear, non-convex nature of distribution network planning problems [10, 11]. Advanced metaheuristic algorithms, including the sine-cosine algorithm (SCA) and the Newton metaheuristic algorithm (NMA), have proven particularly effective in navigating these high-dimensional search spaces, offering superior convergence and solution quality compared to conventional methods [7,8]. Recent innovations such as the atan-sinc optimization algorithm (ASOA) further demonstrate the continued evolution of computational tools for coordinated resource allocation [12].

Contemporary research trends encompass three key directions: the refinement of optimization algorithms for device allocation, the development of hybrid methodologies combining metaheuristic search with analytical sensitivity indices, and the exploration of smart inverter topologies enabling dual-mode PV-STATCOM operation [13, 14]. Collectively, these advances establish a robust technical foundation for achieving annual operating cost reductions of approximately 35% in standard test networks while enhancing voltage profiles and system reliability [8, 9].

This work presents a new hierarchical optimization architecture for the coordinated allocation of PVs and D-STATCOMs in medium-voltage distribution networks, addressing both their optimal locations and capacities. The primary contribution of this study lies in the systematic evaluation and performance validation of the NMA—originally developed for structural engineering applications [15]—in the context of mixed-integer nonlinear programming (MINLP) problems related to power distribution system planning. The upper level of this framework employs the NMA, a recently introduced metaheuristic that combines gradient-based principles with stochastic search mechanisms in order to explore solution spaces through a mixed-variable formulation. Within this formulation, integer decision variables select candidate installation buses for both technologies, while continuous variables establish their optimal power ratings. The lower-level component utilizes a multi-period iterative power flow solver based on successive approximations to verify the operational viability of each design, ensuring adherence to nodal voltage limits and correct active and reactive power injections by compensation devices under realistic loading and generation scenarios.

The NMA is particularly well-suited for this problem due to its distinctive search characteristics. The algorithm maintains a hybrid balance between exploration and exploitation through a time-dependent weighting mechanism ($t/t_{\max}$), which progressively transitions from global exploration in early iterations to localized exploitation as the search converges. Additionally, the NMA incorporates a gradient-inspired term Γ that guides the search direction based on relative solution quality, enabling a more efficient navigation of the non-convex, multi-modal search space of MINLP problems. These features collectively enhance the algorithm's ability to escape local optima—a known challenge in PV and D-STATCOM placement problems—while maintaining computational efficiency.

Methodologically, this research integrates realistic operational and environmental data to ensure practical relevance. Network load characteristics are modeled using actual demand profiles—measured values for the daily active and reactive power consumption at the substation—provided by the utility. Similarly, PV generation patterns are constructed by processing long-term solar irradiance records in order to obtain a region-specific power production curve for the analyzed feeder. To establish a rigorous performance baseline, benchmark methods including the vortex search algorithm (VSA) [9] and the SCA [8] are executed under the same simulation environment and constraints.

This comparative analysis demonstrates that the NMA achieves superior solution quality and convergence behavior, with annual operating cost reductions of up to 35.67% on standard 33- and 69-bus test systems. This performance improvement is attributed to the NMA's effective handling of the discrete-continuous solution space and its robust exploration mechanism, which together yield economically optimal configurations that benchmark

algorithms fail to identify. Our simulation results confirm the effectiveness of the proposed optimizer, positioning the NMA as a robust and efficient tool for planning distributed energy resource integration in modern distribution systems.

The remainder of this document is structured as follows. Section 2 formulates the mathematical optimization model for the joint placement and sizing of PVs and D-STATCOMs in radial distribution networks. The problem is formulated as a MINLP model aimed at minimizing the total annualized investment and operating costs over a 20-year planning period. Section 3 describes the proposed master–slave solution methodology, wherein the NMA is combined with a multi-period power flow solver to address the computational challenges of the MINLP model. Section 4 details the simulation setup, including the 33- and 69-bus test systems, the parameterization of objective functions and operational constraints, and the input data related to demand and generation profiles. Section 5 reports and discusses the numerical results, validating the performance of the proposed approach and comparing its results against those obtained from benchmark methods reported in the literature. Finally, Section 6 summarizes the main contributions of this work and provides recommendations for future work regarding the integration of distributed energy resources.

2. Mathematical formulation

This section presents a comprehensive MINLP model for the strategic integration of PVs and D-STATCOMs into electrical networks. The framework simultaneously optimizes siting, sizing, and operational setpoints to minimize lifetime costs while satisfying technical constraints [16].

2.1. Cost minimization framework

Our model aims to minimize the system's total annualized cost, composed of three primary components: energy procurement from the upstream grid, capital investment in PV and D-STATCOM units, and ongoing operation and maintenance costs [9]. This objective is expressed as follows:

$$\min\ C_{\text{TOTAL}} = C_{\text{GRID}} + C_{\text{PV}}^{\text{invest}} + C_{\text{PV}}^{\text{O\&M}} + C_{\text{D-STATCOM}}, \tag{1}$$

where

$$C_{\text{GRID}} = C_{kWh} \cdot T \cdot f_a \cdot f_c \sum_{h\in\mathcal{H}} \sum_{i\in\mathcal{N}} p_{i,h}^{cg} \Delta h, \tag{2}$$

represents the present value of energy purchased from the central grid over the planning horizon,

$$C_{\text{PV}}^{\text{invest}} = C_{pv} \cdot f_a \sum_{i\in\mathcal{N}} p_i^{pv}, \tag{3}$$

denotes the annualized capital cost of the installed PV capacity,

$$C_{\text{PV}}^{\text{O\&M}} = T \sum_{h\in\mathcal{H}} \sum_{i\in\mathcal{N}} C_{O\&M}^{pv} p_{i,h}^{pv} \Delta h, \tag{4}$$

captures the total operation and maintenance costs for PVs across all periods, and

$$C_{\text{D-STATCOM}} = \gamma \sum_{i\in\mathcal{N}} \left(\omega_1 (q_i^{comp})^3 + \omega_2 (q_i^{comp})^2 + \omega_3 q_i^{comp}\right) \tag{5}$$

models the cubic investment cost for D-STATCOM units based on their reactive power rating.

2.2. Constraints

To ensure feasible and physically realistic solutions, the optimization model incorporates the following technical and operational constraints, categorized by their physical interpretation:

2.2.1. Nodal power balance constraints The AC power flow equations that enforce the conservation of active and reactive power at each bus are defined below:

$$p_{i,h}^{cg} + p_{i,h}^{pv} - P_{i,h}^{d} = \sum_{j \in \mathcal{N}} v_{i,h}\, v_{j,h}\, Y_{ij}\, \cos\big(\theta_{i,h} - \theta_{j,h} - \varphi_{ij}\big), \qquad \forall i \in \mathcal{N},\ h \in \mathcal{H}, \tag{6}$$

$$q_{i,h}^{cg} + q_{i,h}^{comp} - Q_{i,h}^{d} = \sum_{j \in \mathcal{N}} v_{i,h}\, v_{j,h}\, Y_{ij}\, \sin\big(\theta_{i,h} - \theta_{j,h} - \varphi_{ij}\big), \qquad \forall i \in \mathcal{N},\ h \in \mathcal{H}, \tag{7}$$

where Y_{ij} and φ_{ij} denote the magnitude and phase angle of the admittance between buses i and j.

2.2.2. Generation and compensation capability limits The operational ranges of conventional generation, PVs, and reactive compensators are enforced through the following bounds:

$$P_i^{cg,\min} \le p_{i,h}^{cg} \le P_i^{cg,\max}, \qquad \forall i \in \mathcal{N},\ h \in \mathcal{H}, \tag{8}$$

$$Q_i^{cg,\min} \le q_{i,h}^{cg} \le Q_i^{cg,\max}, \qquad \forall i \in \mathcal{N},\ h \in \mathcal{H}, \tag{9}$$

$$p_{i,h}^{pv} = G_{i,h}^{pv}\, p_i^{pv}, \qquad \forall i \in \mathcal{N},\ h \in \mathcal{H}, \tag{10}$$

$$x_i^{pv}\, P^{pv,\min} \le p_i^{pv} \le x_i^{pv}\, P^{pv,\max}, \qquad \forall i \in \mathcal{N}, \tag{11}$$

$$x_i^{comp}\, Q^{comp,\min} \le q_i^{comp} \le x_i^{comp}\, Q^{comp,\max}, \qquad \forall i \in \mathcal{N}, \tag{12}$$

$$q_{i,h}^{comp} = q_i^{comp}, \qquad \forall i \in \mathcal{N},\ h \in \mathcal{H}. \tag{13}$$

Constraint (10) couples the installed PV capacity p_i^{pv} with the actual generation $p_{i,h}^{pv}$ via the time-varying solar availability factor $G_{i,h}^{pv}$.

2.2.3. Network security and installation constraints Voltage profile integrity and practical limits on the number of installed devices are enforced by

$$v^{\min} \le v_{i,h} \le v^{\max}, \qquad \forall i \in \mathcal{N},\ h \in \mathcal{H}, \tag{14}$$

$$\sum_{i \in \mathcal{N}} x_i^{pv} \le N_{pv}^{ava}, \tag{15}$$

$$\sum_{i \in \mathcal{N}} x_i^{comp} \le N_{comp}^{ava}. \tag{16}$$

Inequalities (15) and (16) restrict the total number of PVs and D-STATCOMs that can be installed in the network.

2.2.4. Economic parameters The annualization factor f_a and the energy-cost escalation factor f_c, which appear in the objective function, are computed based on the following financial parameters:

$$f_a = \frac{r_a}{1 - (1 + r_a)^{-N_y}}, \tag{17}$$

$$f_c = \sum_{t=1}^{N_y} \left(\frac{1 + r_e}{1 + r_a} \right)^t, \tag{18}$$

where r_a denotes the annual discount rate, r_e the annual escalation rate of energy prices, and N_y the total number of years in the planning horizon.

2.3. Mathematical structure and problem classification

The optimization model presented in Equations (1)-(18) exhibits a complex mathematical structure that merits detailed analysis. This section examines the key characteristics that define the problem's computational complexity and solution challenges.

2.3.1. MINLP structure The formulation constitutes a canonical MINLP problem due to the simultaneous presence of:

- **Continuous variables**: power flows $(p_{i,h}^{cg}, q_{i,h}^{cg})$, voltage magnitudes $v_{i,h}$, PV generation $p_{i,h}^{pv}$, and compensation levels $q_{i,h}^{comp}$
- **Discrete variables**: binary installation decisions (x_i^{pv} and x_i^{comp})
- **Nonlinear relationships**: trigonometric functions in the power flow equations and polynomial terms in the objective function

This combination results in an NP-hard problem, requiring specialized solution approaches beyond traditional linear or convex optimization techniques.

2.3.2. Non-convex components The model contains several inherently non-convex elements that significantly impact the solution strategy:

- **Power flow equations**: Constraints (6) and (7) introduce non-convexity through the product terms $v_{i,h}v_{j,h}$ and the trigonometric functions $\cos(\cdot)$ and $\sin(\cdot)$. These equations define a non-convex feasible region that may contain multiple local optima.
- **Cubic cost function**: The D-STATCOM investment cost in Equation (1) includes a cubic term $\omega_1(q_i^{comp})^3$, which is non-convex for positive ω_1 values—typically encountered in practical applications.

2.3.3. Convex and linear components Despite the generalized non-convexity, several model elements exhibit convex or linear structures:

- **Linear inequality constraints**: the Generation Bounds (8) and (9), the Voltage Limits (14), and the Installation Limits (15) and (16) define convex polyhedral regions.
- **Linear equality constraints**: the fixed compensation dispatch $q_{i,h}^{comp} = q_i^{comp}$ in Equation (13) represents an affine relationship.
- **Linear objective components**: the energy purchase costs C_{GRID} and the PV O&M costs $C_{\text{PV}}^{\text{O\&M}}$ are linear functions of their corresponding variables.

2.3.4. Multi-period temporal coupling The inclusion of time index $h \in \mathcal{H}$ introduces temporal dependencies that

- increase problem dimensionality by a factor of $|\mathcal{H}|$.
- create inter-temporal linkages through investment decisions that persist across all time periods.
- require the consideration of time-varying parameters ($G_{i,h}^{pv}$, $P_{i,h}^{d}$, $Q_{i,h}^{d}$) that reflect daily and seasonal variations.

This temporal dimension transforms a static placement problem into one involving dynamic optimization, requiring solutions that remain feasible across all operating conditions.

2.3.5. Problem decomposition potential The formulation's inherent master-slave structure suggests some natural decomposition opportunities:

- The **master problem** handles discrete installation decisions (x_i^{pv}, x_i^{comp}) and continuous sizing variables (p_i^{pv}, q_i^{comp}).
- The **slave problem** solves the multi-period optimal power flow for a set of given installation configurations, evaluating their technical feasibility and operating costs.

This decomposition aligns well with metaheuristic approaches, wherein the master problem can be addressed through stochastic search methods while the slave problem employs deterministic power flow algorithms.

The next section presents a tailored algorithmic framework designed to address these mathematical challenges while efficiently solving the integrated siting and sizing problem for PVs and D-STATCOMs.

3. Solution approach

This section presents the two-phase computational framework developed to solve the MINLP model defined in Section 2. Our approach employs a hierarchical master-slave architecture that decouples investment decisions from the operational validation, thereby addressing the inherent complexity of the integrated planning problem. In the upper (master) level, the NMA explores the combinatorial space of installation locations and device capacities. For each candidate configuration proposed by the master level, the lower (slave) level executes a specialized power flow analysis to verify technical feasibility and compute precise operating costs. This decomposition enables an efficient navigation of the high-dimensional, non-convex search space while ensuring that all physical and operational constraints are satisfied. The subsequent subsections elaborate on each component of this methodology.

3.1. Lower-level optimization: power flow validation

The lower-level (slave) component of the solution framework implements a specialized power flow solver to evaluate the technical feasibility of each candidate configuration generated by the master stage. This module solves the nonlinear power balance equations using the complex-domain successive approximations method. For a given set of installation decisions and device capacities, the solver computes the corresponding voltage profiles across all network buses and time periods while ensuring that all operational constraints are satisfied.

3.1.1. Matrix-based power flow formulation The core iterative equation implementing the successive approximations method is expressed below [17]:

$$\mathbf{V}_{d,h}^{(k+1)} = -\mathbf{Y}_{dd}^{-1}\left[\text{diag}^{-1}\left(\mathbf{V}_{d,h}^{(k)*}\right)\mathbf{S}_{d,h}^{*} - \mathbf{Y}_{dg}\mathbf{V}_{g,h}\right], \quad \forall h \in \mathcal{H}, \tag{19}$$

where the superscript (k) denotes the iteration index. In this formulation,

- $\mathbf{V}_{d,h}^{(k+1)}$ is the vector of complex voltages at the demand nodes for time period h at iteration $k+1$.
- $\mathbf{Y}_{dd}^{-1}$ denotes the inverse of the demand-node submatrix of the nodal admittance matrix.
- $\mathbf{S}_{d,h}^{*}$ represents the net complex power injection at the demand nodes, calculated as

  $$\mathbf{S}_{d,h}^{*} = \mathbf{S}_{d,h}^{dg} + \mathbf{S}_{h}^{pv} + j\mathbf{S}_{h}^{comp} - \mathbf{S}_{d,h}^{load}.$$

  The terms $\mathbf{S}_{h}^{pv}$ and $\mathbf{S}_{h}^{comp}$ correspond to active power from PVs and reactive power from D-STATCOMs, respectively, while $\mathbf{S}_{d,h}^{load}$ captures the nodal power demand.
- $\mathbf{Y}_{dg}$ is the coupling submatrix of the admittance matrix between the demand nodes and the slack bus.
- $\mathbf{V}_{g,h}$ is the fixed complex voltage at the slack bus, typically set to the nominal substation voltage.

3.1.2. Convergence criterion The iterative process terminates when the maximum voltage difference between consecutive iterations falls below a prescribed tolerance ϵ, thereby ensuring numerical stability and accuracy. The convergence criterion is defined as follows [18]:

$$\max_{i \in \mathcal{N}} \left|\mathbf{V}_{i,h}^{(k+1)} - \mathbf{V}_{i,h}^{(k)}\right| \leq \epsilon, \quad \forall h \in \mathcal{H}, \tag{20}$$

where $\epsilon = 1 \times 10^{-10}$ in this implementation.

3.1.3. Slack bus power calculation Upon convergence, the complex power injection at the substation (slack bus) for each time period is computed in order to validate the global power balance:

$$\mathbf{S}_{g,h} = \mathbf{Y}_{dg}\mathbf{V}_{g,h} + \mathbf{Y}_{gd}\mathbf{V}_{d,h}, \quad \forall h \in \mathcal{H}, \tag{21}$$

where $\mathbf{S}_{g,h}$ denotes the complex power supplied by the slack bus during period h, and $\mathbf{Y}_{gd}$ is the transpose of $\mathbf{Y}_{dg}$. This calculation provides the final grid energy consumption required for cost evaluation in the Objective Function (1).

3.1.4. Feasibility assessment The power flow solution constitutes the core feasibility check within the master-slave framework. A candidate configuration is only deemed feasible if (i) the iterative process converges according to (20) and (ii) all resulting voltage magnitudes satisfy the regulatory bounds defined in (14). Any violation of either condition triggers a penalty mechanism in the master stage, steering the search towards technically admissible solutions.

3.2. Upper-level optimization: NMA approach

The NMA is a recently developed population-based optimization technique that hybridizes gradient-informed search mechanisms with stochastic exploration strategies [15]. Originally formulated for the discrete performance-based seismic design of steel structures, it adapts the classical Newton method—a deterministic, gradient-based approach—into a metaheuristic framework suitable for navigating complex, high-dimensional, and non-convex search spaces. The algorithm maintains a population of candidate solutions, each updated using a direction that combines local gradient information with guidance from the best solution discovered by the population [19]. This hybridization allows for an effective balance between intensification (exploiting promising regions) and diversification (exploring the global search space), a critical requirement for solving challenging MINLP problems. In the following subsections, the core mechanics of the NMA are detailed, along with its adaptation to the discrete–continuous optimization structure inherent to the problem under study.

3.2.1. Solution representation and initial population The mathematical encoding of potential solutions is a crucial component of the metaheuristic optimization process. In this work, each candidate solution is represented as a vector that simultaneously encodes the location and capacity of PV and D-STATCOM units within the distribution network. To illustrate this, consider a 33-bus test system where two PV units and two D-STATCOMs are to be optimally allocated, with maximum allowable capacities of 1500 kW and 1200 kvar, respectively. A representative solution vector would be structured as follows:

$$\mathbf{x}_j = \big[\ \underbrace{5,\ 18}_{\text{PV nodes}} \quad \underbrace{10,\ 28}_{\text{D-STATCOM nodes}} \quad \underbrace{876.32,\ 1341.50}_{\text{PV sizes (kW)}} \quad \underbrace{430.20,\ 985.40}_{\text{D-STATCOM sizes (kvar)}}\ \big]. \tag{22}$$

The interpretation of this vector is twofold:

1. The first two integer entries (5 and 18) specify the bus locations for the PVs, with the subsequent two entries (10 and 28) indicating the installation buses for the D-STATCOMs.
2. The remaining four real-valued entries correspond to the rated capacities of the devices in the order of their placement: 876.32 kW and 1341.50 kW for the PVs, and 430.20 kvar and 985.40 kvar for the reactive compensators.

The solution vector $\mathbf{x}_j$ corresponds to the j-th individual in a population of size n_s at iteration p. The complete population is organized as a matrix $\mathbf{X}^t \in \mathbb{R}^{n_s \times n_v}$, where n_v denotes the total number of decision variables (including both discrete location indices and continuous size parameters). This hybrid discrete-continuous encoding allows for a unified representation that can be efficiently manipulated by the metaheuristic search operators.

The initial population $\mathbf{X}^0$ is generated by sampling each decision variable uniformly within its prescribed bounds. For the l-th variable of the j-th candidate solution, the initialization rule is as follows:

$$x_{j,l}^0 = x_l^{\min} + \beta_{j,l}\big(x_l^{\max} - x_l^{\min}\big), \qquad \begin{cases} l = 1, 2, \ldots, n_v, \\ j = 1, 2, \ldots, n_s, \end{cases} \tag{23}$$

where $\beta_{j,l} \sim \mathcal{U}[0,1]$ is a uniformly distributed random number, and $[x_l^{\min},\ x_l^{\max}]$ defines the admissible range for the l-th variable. For the location variables, the bounds are the minimum and maximum bus indices (*e.g.*, 2 and 33 in a 33-bus network). For the capacity variables, they correspond to the technical limits of the devices. This randomized yet bounded initialization ensures diversity across the initial population while guaranteeing that every candidate solution resides within the feasible search space, thereby promoting a robust exploration during the early stages of the optimization process.

3.2.2. Equilibrium between exploration and exploitation A fundamental aspect of an effective metaheuristic search is the balanced interplay between the global exploration of the solution space and the local refinement of promising regions. The NMA achieves this balance through a dynamic update rule that integrates gradient-informed movement with stochastic diversification.

Elite solution selection At each iteration t, the population $\mathbf{X}^t$ is evaluated via a fitness function $F_f(\cdot)$ that encodes both the economic objective and constraint satisfaction. The elite candidate $\mathbf{x}_{\text{best}}^t$—corresponding to the fittest individual in the current population—is identified as follows:

$$x_{\text{best}}^t = \left\{ x_j^t \mid x_j^t = \arg\min \left(F_f \left(x_j^t \right) \right), \ \forall j = 1, 2, \ldots, n_s \right\}, \tag{24}$$

where $\mathbf{x}_j^t$ denotes the j-th candidate solution at iteration p. The elite solution guides the search direction and serves as an attractor in the subsequent updating process.

Penalized fitness evaluation To handle the inequality constraints inherent in the MINLP formulation, a barrier penalty method is employed. The fitness function combines the original objective with a weighted measure of constraint violation:

$$F_f(\mathbf{x}) = C_{\text{TOTAL}}(\mathbf{x}) + \sum_{k=1}^{K} \lambda_k \cdot \max \left\{ g_k(\mathbf{x}), \, 0 \right\}, \tag{25}$$

where $C_{\text{TOTAL}}(\mathbf{x})$ is the total cost defined in (1), $g_k(\mathbf{x}) \leq 0$ represents the k-th inequality constraint, and $\lambda_k > 0$ is the corresponding penalty coefficient. The term $\max\{g_k(\mathbf{x}), 0\}$ quantifies the violation of constraint k: feasible solutions yield zero penalty, while infeasible ones are penalized proportionally to the magnitude of their violation. A proper calibration of the penalty coefficients λ_k ensures that the search is systematically directed towards feasible regions without premature convergence to suboptimal solutions.

Dynamic update mechanism The core search strategy of the NMA is governed by an evolution rule that adaptively combines stochastic exploration with gradient-informed exploitation. For the j-th candidate solution at iteration t, the update equation is given by [15]:

$$\mathbf{y}_j^t = \mathbf{x}_j^t + \frac{t}{t_{\max}} r_1 \, \Gamma \left(\mathbf{x}_{j-1}^t - \mathbf{x}_{j+1}^t \right) + \left(1 - \frac{t}{t_{\max}} \right) r_2 \left(\mathbf{x}_{\text{best}}^t - \mathbf{x}_j^t \right), \tag{26}$$

where:

- $\mathbf{y}_j^t$ is the updated solution for the next iteration
- $t_{\max}$ denotes the maximum allowable number of iterations
- $r_1, r_2 \sim \mathcal{U}[0, 1]$ are independent, uniformly distributed random numbers
- $\mathbf{x}_{\text{best}}^t$ represents the best solution found as of iteration t (*i.e.*, the solution yielding the lowest objective function value)
- Γ is a gradient-like term that approximates the local curvature of the objective landscape

The term Γ is computed using a finite-difference approximation based on three consecutive candidate solutions:

$$\Gamma = \frac{\tau^2 f\left(\mathbf{x}_{j+1}^t\right) + (1 - 2\tau) f\left(\mathbf{x}_j^t\right) - (1 - \tau)^2 f\left(\mathbf{x}_{j-1}^t\right)}{2\tau f\left(\mathbf{x}_{j+1}^t\right) - 2 f\left(\mathbf{x}_j^t\right) + 2 (1 - \tau) f\left(\mathbf{x}_{j-1}^t\right)}, \tag{27}$$

where $f(\cdot)$ denotes the objective (fitness) function evaluated for the corresponding solution vector, and τ is a relative distance ratio defined as

$$\tau = \frac{\left\| \mathbf{x}_j^t - \mathbf{x}_{j-1}^t \right\|}{\left\| \mathbf{x}_{j+1}^t - \mathbf{x}_{j-1}^t \right\|}. \tag{28}$$

Note that the interpretation of the update rule given in Equation (26) embodies a time-varying balance between two components:

- The first term, weighted by $t/t_{\max}$, promotes exploration by introducing a stochastic perturbation scaled by the gradient-like factor Γ. Early in the search ($t \ll t_{\max}$), this term is dominant, encouraging a diverse sampling of the solution space.
- The second term, weighted by $1 - t/t_{\max}$, drives exploitation by attracting the current solution towards the elite individual $\mathbf{x}_{\text{best}}^t$. As t approaches $t_{\max}$, this attraction becomes predominant, refining solutions in the vicinity of the best-known region.

The gradient-inspired factor Γ, derived from a quadratic interpolation of the objective function over three neighboring solutions, provides a local approximation of the Newton direction, thereby accelerating convergence near promising regions. This hybrid mechanism allows the NMA to effectively navigate the complex, non-convex search space of integrated PV and D-STATCOM planning problems.

To maintain technical feasibility, every solution produced by the NMA is projected onto the admissible hyper-rectangle defined by the variable bounds. Each decision variable $x_{j,l}^{t+1}$ is constrained as follows:

$$y_{j,l}^t \leftarrow \max\left(x_l^{\min}, \min\left(y_{j,l}^t, x_l^{\max}\right)\right).$$

This simple yet essential step ensures that all candidate designs respect the inherent physical limits of the network, enabling their subsequent evaluation via the power-flow solver in the slave stage without failures associated with infeasibility.

3.2.3. Population substitution After generating the new candidate solutions, denoted by y_j^t, it is necessary to decide whether they will be included in the population for the next iteration. To this effect, the performance function value $F_f\left(y_j^t\right)$ must be evaluated. Based on this value, the replacement rule for the population is defined as follows:

$$x_j^{t+1} = \begin{cases} y_j^t, & F_f\left(y_j^t\right) < F_f\left(x_j^t\right) \\ x_j^t, & F_f\left(y_j^t\right) \geq F_f\left(x_j^t\right) \end{cases}, \quad \forall j = 1, 2, ..., n_s. \tag{29}$$

This rule allows updating the population by replacing existing solutions with new candidates if they perform better according to the fitness function.

3.2.4. Termination conditions The iterative search process of the NMA concludes when one of two standard convergence criteria is satisfied. These criteria are designed to balance computational efficiency with solution quality, preventing both premature termination and excessive runtime.

Maximum iteration limit A predefined iteration ceiling $t_{\max}$ is established prior to execution. Once the algorithm completes $t_{\max}$ cycles, the search halts and returns the best solution found. This criterion ensures a finite computational budget.

Stagnation detection To avoid unnecessary iterations after convergence, a stagnation counter κ tracks successive cycles without improvement in the elite solution's fitness. The process terminates if

$$\kappa \geq \kappa_{\max},$$

where $\kappa_{\max}$ is a user-defined tolerance, typically set between 10% and 30% of $t_{\max}$. This condition indicates that the search has likely reached a stable region, and further iterations yield diminishing returns.

Both criteria are commonly adopted in metaheuristic optimization to ensure a principled balance between exploration depth and computational expenditure. In this work, the algorithm terminates when either condition is met, and the incumbent best solution $\mathbf{x}_{\text{best}}$ is reported as the final design.

4. Experimental setup

To evaluate the performance of our proposed hierarchical optimization framework, numerical simulations were conducted using two classical radial distribution test systems comprising 33 and 69 buses. The topology and electrical parameters of these feeders, which are widely adopted as benchmarks in distribution system planning studies, are illustrated in Figure 1 and summarized in Table 1. Both systems are configured as radial networks with a nominal substation voltage of 12.66 kV. In accordance with standard operational practices, the nodal voltage magnitudes are constrained to remain within $\pm 10\%$ of the nominal value throughout all simulations [20]. This experimental configuration provides a controlled yet realistic environment for assessing the efficacy of the integrated Newton metaheuristic and power-flow methodology in solving the joint PV and D-STATCOM planning problem.

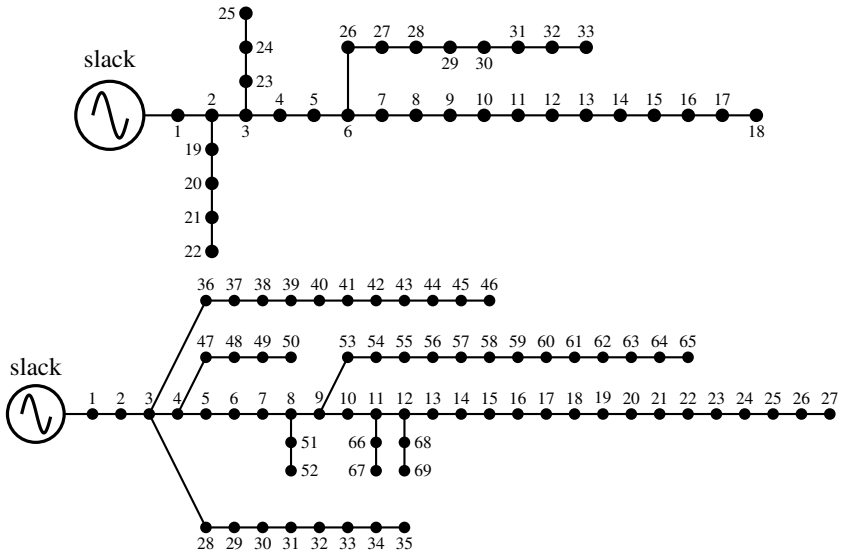

Figure 1. Network topologies employed for numerical validation: (upper) 33-bus feeder and (lower) 69-bus feeder

The performance assessment of the proposed planning methodology utilized representative daily operational profiles for both load consumption and solar resource availability. These profiles, which capture the time-varying nature of power demand and renewable generation, are essential for evaluating the robustness of PV and D-STATCOM allocations under realistic operating conditions.

Figure 2 presents the normalized daily curves employed in the simulations. The active and reactive power demand profiles (derived from actual utility measurements) exhibit characteristic residential/commercial patterns with morning ramp-ups, midday plateaus, and evening peaks. Concurrently, the solar generation profile follows a bell-shaped trajectory typical of clear-sky conditions, reaching its peak during the midday hours and decaying to zero during nighttime.

These complementary datasets enable a comprehensive evaluation of the optimization framework's ability to handle the inherent variability and intermittency of renewable resources while maintaining grid stability and minimizing operating costs.

The economic analysis considered within the optimization model incorporates specific financial and technical coefficients for both PVs and reactive compensators. These parameters, detailed in Tables 2 and 3, directly inform the cost calculation components of the objective function defined in Equation (1). The PV-related values encompass energy pricing, capital investment, operating costs, and project lifetime considerations. For D-STATCOMs, the cost structure is characterized by a cubic polynomial relating reactive power capacity to investment outlay, with additional parameters specifying permissible operating ranges for both compensators and conventional generation sources.

Table 1. Feeder specifications, including branch impedances and active/reactive power demands for both test networks

33-bus grid											
Node i	**Node j**	**R_{ij} (Ω)**	**X_{ij} (Ω)**	**P_j (kW)**	**Q_j (kvar)**	**Node i**	**Node j**	**R_{ij} (Ω)**	**X_{ij} (Ω)**	**P_j (kW)**	**Q_j (kvar)**
1	2	0.0922	0.0477	100	60	17	18	0.7320	0.5740	90	40
2	3	0.4930	0.2511	90	40	2	19	0.1640	0.1565	90	40
3	4	0.3660	0.1864	120	80	19	20	1.5042	1.3554	90	40
4	5	0.3811	0.1941	60	30	20	21	0.4095	0.4784	90	40
5	6	0.8190	0.7070	60	20	21	22	0.7089	0.9373	90	40
6	7	0.1872	0.6188	200	100	3	23	0.4512	0.3083	90	50
7	8	1.7114	1.2351	200	100	23	24	0.8980	0.7091	420	200
8	9	1.0300	0.7400	60	20	24	25	0.8960	0.7011	420	200
9	10	1.0400	0.7400	60	20	6	26	0.2030	0.1034	60	25
10	11	0.1966	0.0650	45	30	26	27	0.2842	0.1447	60	25
11	12	0.3744	0.1238	60	35	27	28	1.0590	0.9337	60	20
12	13	1.4680	1.1550	60	35	28	29	0.8042	0.7006	120	70
13	14	0.5416	0.7129	120	80	29	30	0.5075	0.2585	200	600
14	15	0.5910	0.5260	60	10	30	31	0.9744	0.9630	150	70
15	16	0.7463	0.5450	60	20	31	32	0.3105	0.3619	210	100
16	17	1.2860	1.7210	60	20	32	33	0.3410	0.5302	60	40
69-bus grid											
Node i	**Node j**	**R_{ij} (Ω)**	**X_{ij} (Ω)**	**P_j (kW)**	**Q_j (kvar)**	**Node i**	**Node j**	**R_{ij} (Ω)**	**X_{ij} (Ω)**	**P_j (kW)**	**Q_j (kvar)**
1	2	0.0005	0.0012	0.00	0.00	3	36	0.0044	0.0108	26.00	18.55
2	3	0.0005	0.0012	0.00	0.00	36	37	0.0640	0.1565	26.00	18.55
3	4	0.0015	0.0036	0.00	0.00	37	38	0.1053	0.1230	0.00	0.00
4	5	0.0251	0.0294	0.00	0.00	38	39	0.0304	0.0355	24.00	17.00
5	6	0.3660	0.1864	2.60	2.20	39	40	0.0018	0.0021	24.00	17.00
6	7	0.3810	0.1941	40.40	30.00	40	41	0.7283	0.8509	1.20	1.00
7	8	0.0922	0.0470	75.00	54.00	41	42	0.3100	0.3623	0.00	0.00
8	9	0.0493	0.0251	30.00	22.00	42	43	0.0410	0.0478	6.00	4.30
9	10	0.8190	0.2707	28.00	19.00	43	44	0.0092	0.0116	0.00	0.00
10	11	0.1872	0.0619	145.00	104.00	44	45	0.1089	0.1373	39.22	26.30
11	12	0.7114	0.2351	145.00	104.00	45	46	0.0009	0.0012	29.22	26.30
12	13	1.0300	0.3400	8.00	5.00	4	47	0.0034	0.0084	0.00	0.00
13	14	1.0440	0.3450	8.00	5.50	47	48	0.0851	0.2083	79.00	56.40
14	15	1.0580	0.3496	0.00	0.00	48	49	0.2898	0.7091	384.70	274.50
15	16	0.1966	0.0650	45.50	30.00	49	50	0.0822	0.2011	384.70	274.50
16	17	0.3744	0.1238	60.00	35.00	8	51	0.0928	0.0473	40.50	28.30
17	18	0.0047	0.0016	60.00	35.00	51	52	0.3319	0.1114	3.60	2.70
18	19	0.3276	0.1083	0.00	0.00	9	53	0.1740	0.0886	4.35	3.50
19	20	0.2106	0.0690	1.00	0.60	53	54	0.2030	0.1034	26.40	19.00
20	21	0.3416	0.1129	114.00	81.00	54	55	0.2842	0.1447	24.00	17.20
21	22	0.0140	0.0046	5.00	3.50	55	56	0.2813	0.1433	0.00	0.00
22	23	0.1591	0.0526	0.00	0.00	56	57	1.5900	0.5337	0.00	0.00
23	24	0.3463	0.1145	28.00	20.00	57	58	0.7837	0.2630	0.00	0.00
24	25	0.7488	0.2475	0.00	0.00	58	59	0.3042	0.1006	100.00	72.00
25	26	0.3089	0.1021	14.00	10.00	59	60	0.3861	0.1172	0.00	0.00
26	27	0.1732	0.0572	14.00	10.00	60	61	0.5075	0.2585	1244.00	888.00
3	28	0.0044	0.0108	26.00	18.60	61	62	0.0974	0.0496	32.00	23.00
28	29	0.0640	0.1565	26.00	18.60	62	63	0.1450	0.0738	0.00	0.00
29	30	0.3978	0.1315	0.00	0.00	63	64	0.7105	0.3619	227.00	162.00
30	31	0.0702	0.0232	0.00	0.00	64	65	1.0410	0.5302	59.00	42.00
31	32	0.3510	0.1160	0.00	0.00	11	66	0.2012	0.0611	18.00	13.00
32	33	0.8390	0.2816	14.00	10.00	66	67	0.0470	0.0140	18.00	13.00
33	34	1.7080	0.5646	19.50	14.00	12	68	0.7394	0.2444	28.00	20.00
34	35	1.4740	0.4873	6.00	4.00	68	69	0.0047	0.0016	28.00	20.00

Table 2. Economic and technical parameters governing PV unit planning in distribution grids

Parameter	**Value**	**Unit**	**Parameter**	**Value**	**Unit**
C_{kWh}	0.1390	USD/kWh	T	365	days
t_a	10	%	N_t	20	years
Δh	1	h	t_e	2	%
C_{pv}	1036.49	USD/kWp	C_{0andM}	0.0019	USD/kWh
N_{pv}^{ava}	3	-	$p_i^{pv,\max}$	2400	kW
$P_k^{pv,\min}$	0	kW			

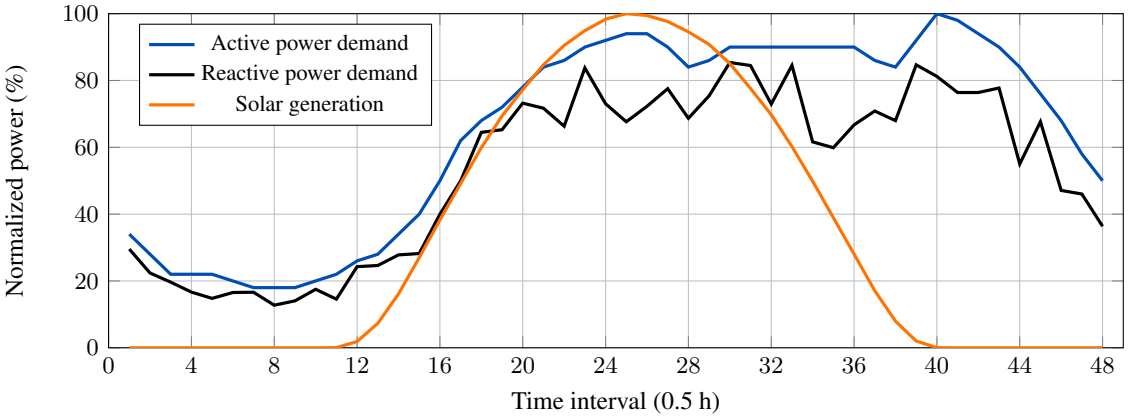

Figure 2. Normalized daily profiles: active/reactive power demand and solar generation potential

Table 3. Economic and operational parameters for reactive power compensator integration

Par.	Value	Unit	Par.	Value	Unit
ω_1	0.30	USD/Mvar^3	ω_2	-305.10	USD/Mvar^2
ω_3	127,380	USD/Mvar	γ	1/20	—
$Q_i^{comp,\min}$	0	Mvar	$Q_{i,h}^{comp,\max}$	2000	kvar
$P_i^{cg,\min}$	0	W	$P_i^{cg,\max}$	5000	kW
$Q_i^{cg,\min}$	0	var	$Q_i^{cg,\max}$	5000	kvar

5. Numerical evaluation

Our master–slave optimization methodology was implemented in MATLAB (version 2024a). All simulations were executed on a desktop computer with an AMD Ryzen 7 3700 processor (2.3 GHz), 16 GB of RAM, and a 64-bit version of Microsoft Windows 10. The implementation included custom scripts for the NMA and a successive approximations power flow solver. To assess its performance, the proposed approach was compared against the VSA [9], the SCA [8], and the ASOA [12].

The test setup imposed the following operational limits: the PV sources were capped at 2400 kW and the D-STATCOMs at 2000 kvar. Each candidate solution could incorporate up to three PVs and three D-STATCOMs. All metaheuristic algorithms employed a population size of 50 individuals and were allowed a maximum of 1000 iterations per run. To ensure statistical reliability, 100 independent executions were performed for each method.

5.1. Numerical validations for the 33-bus grid

Table 4 provides a comparative analysis of the optimization methods applied to the 33-bus distribution network. The results highlight the performance of the NMA, the ASOA, the SCA, and the VSA in reducing project costs, identifying the optimal location of both PVs and D-STATCOMs while evaluating computational efficiency.

Table 4. Performance evaluation on the 33-bus distribution network

Scen.	x_i^{comp} (Node)	q_i^{comp} (Mvar)	x_i^{pv} (Node)	p_i^{pv} (MW)	C_{TOTAL} (USD)	Average time (s)
Benchmark case	—	—	—	—	3,553,557.38	—
VSA	[6, 15, 31]	[0.3801, 0.0640, 0.3543]	[9, 14, 31]	[0.9844, 0.6312, 1.7602]	2,292,022.62	305.36
SCA	[11, 12, 30]	[0.0092, 0.1143, 0.4617]	[7, 14, 31]	[0.4348, 1.8842, 1.0836]	2,291,234.65	305.97
ASOA	[13, 26, 30]	[0.1428, 0.1613, 0.3787]	[11, 16, 31]	[0.8269, 1.3512, 0.4736]	2,290,519.25	311.85
NMA	[7, 15, 30]	[0.0600, 0.1393, 0.4218]	[10, 14, 31]	[0.8996, 0.9306, 1.5570]	2,290,259.24	290.74

Our analysis reveals clear economic and technical performance differences. All metaheuristic approaches (*i.e.*, VSA, SCA, ASOA, and NMA) demonstrated substantial economic improvements with respect to the benchmark,

reducing the annualized project costs by approximately 35.50-35.55%. This significant reduction underscores the value of optimally siting and sizing PVs and D-STATCOMs in order to minimize infrastructure investments and operational losses over the planning horizon.

The NMA achieved the lowest annualized cost (USD 2,290,259.24), outperforming the VSA (USD 2,292,022.62), SCA (USD 2,291,234.65), and ASOA (USD 2,290,519.25). While the cost differences between these metaheuristic methods are relatively small—with a spread of only USD 1,763.38 between the best and worst solutions—, this narrow margin reflects convergence near the region containing the global optimum. However, the NMA's solution represents the most economically efficient configuration, with cost savings of USD 1,763.38 compared to the ASOA and USD 2,259.98 compared to the VSA. When annualized over the 20-year planning period, these savings translate to cumulative present-value benefits that justify the selection of the NMA for practical applications.

An examination of the device allocation strategies reveals important differences in each algorithm's approach to the optimization problem. Bus 31 emerges as a consistently critical node across all solutions, being selected for either PV or D-STATCOM placement in every algorithm—and simultaneously for both technologies in the case of the VSA. This consensus indicates that bus 31, located at the far end of the main feeder, is electrically disadvantaged and requires compensation to maintain its voltage within acceptable limits. The NMA places a 1.5570 MW PV system at this bus, providing active power injection that directly addresses the voltage drop characteristic of radial network endpoints. In contrast, the VSA places both a PV (1.7602 MW) and a D-STATCOM (0.3543 Mvar) at bus 31, representing a more capital-intensive approach to addressing the same underlying issue.

Bus 14 is another strategically important location, selected by the NMA, VSA, and SCA for PV placement. This bus sits at a junction point where power flows diverge towards multiple lateral branches. The NMA allocates 0.9306 MW at this location, while the SCA allocates a substantially larger 1.8842 MW and the VSA a more modest 0.6312 MW. The variation in allocated capacities reflects different trade-offs between local generation benefits and system-wide losses reduction. The NMA's intermediate allocation suggests a balanced approach that captures the benefits of distributed generation without over-concentrating capacity at any single node.

The D-STATCOM placement patterns exhibit greater variation across algorithms. The VSA places a large compensator (0.3801 Mvar) at bus 6, which is electrically close to the substation, while the NMA places its largest compensator (0.4218 Mvar) at bus 30, near the feeder endpoint. This difference reflects distinct compensation philosophies: upstream compensation provides system-wide voltage support but may not address localized voltage problems at distal nodes, while downstream compensation directly targets the most voltage-sensitive locations. The NMA's strategy of placing the largest compensator at bus 30, complemented by moderate compensation at bus 15 (0.1393 Mvar) and a smaller unit at bus 7 (0.0600 Mvar), creates a tiered support structure that addresses both localized needs and system-wide voltage regulation.

The SCA presents an interesting contrast with very small D-STATCOM at bus 11 (0.0092 Mvar) and bus 12 (0.1143 Mvar), suggesting that this algorithm prioritizes PV placement for voltage support while using D-STATCOMs primarily for fine-tuning. The ASOA distributes its D-STATCOMs more evenly across buses 13, 26, and 30, with capacities ranging from 0.1428 to 0.3787 Mvar. This represents a middle ground between the VSA's upstream focus and the NMA's downstream emphasis.

A decisive advantage of the NMA is its superior computational efficiency, reporting the shortest average execution time (290.74 seconds). This represents a 4.8% reduction compared to the VSA (305.36 s), 5.0% compared to the SCA (305.97 s), and 6.8% compared to the ASOA (311.85 s). This performance gain, coupled with its superior economic outcomes, confirms the NMA's robustness and effectiveness for practical planning applications. The algorithm's faster convergence, which does not compromise solution quality, makes it particularly suitable for real-world planning studies where repeated simulations and time-sensitive analyses are required.

The combination of low-cost operation, strategic device placement, and superior computational efficiency positions the NMA as the most effective optimization method among those evaluated for the 33-bus system. While all algorithms produce solutions within a narrow economic range, the NMA's ability to identify a configuration that balances upstream and downstream compensation while minimizing execution time demonstrates the practical advantages of its search mechanism.

5.2. Numerical validations for the 69-bus grid

The numerical results for the larger 69-bus distribution network, which are presented in Table 5, confirm and reinforce the performance trends observed in the 33-bus case. All optimization algorithms achieved substantial economic savings compared to the benchmark, reducing the total costs by approximately 35.5-35.7%. This consistent improvement across both test systems demonstrates the universal value of optimal device placement for grid planning. Once again, the NMA achieved the lowest total cost (USD 2,395,022.55), with reductions ranging from USD 1,298 to USD 5,468 relative to the other methods.

Table 5. Performance evaluation on the 69-bus distribution network

Scen.	x_i^{comp} **(Node)**	q_i^{comp} **(Mvar)**	x_i^{pv} **(Node)**	p_i^{pv} **(MW)**	C_{TOTAL} **(USD)**	**Average time (s)**
Benchmark case	—	—	—	—	3,723,529.52	—
VSA	[19, 53, 63]	[0.0871, 0.0075, 0.4555]	[15, 33, 62]	[0.8753, 0.5941, 2.0184]	2,400,490.65	1680.10
SCA	[7, 61, 65]	[0.0337, 0.3992, 0.1076]	[18, 59, 61]	[0.8761, 0.3407, 2.2949]	2,396,720.37	1611.16
ASOA	[16, 61, 64]	[0.0613, 0.4481, 0.0835]	[61, 62, 64]	[1.5558, 1.2796, 0.7524]	2,395,320.95	1675.35
NMA	[15, 61, 64]	[0.0979, 0.4279, 0.1217]	[17, 61, 62]	[0.4551, 1.3118, 1.7695]	2,395,022.55	1393.39

These device allocation strategies reveal distinct optimization patterns. The NMA places D-STATCOMs at buses 15, 61, and 64, with reactive power compensation values between 0.0979 and 0.4279 Mvar, and it positions PVs at buses 17, 61, and 62, with a balanced power injection profile totaling 3.5364 MW. This configuration demonstrates effective resource diversification, avoiding concentration at single nodes while maintaining technical feasibility. Notably, the ASOA concentrates all three PV units in a tight cluster (buses 61, 62, and 64), which may pose operational risks, whereas the NMA's more distributed approach likely enhances system resilience and voltage support.

When examining the placement patterns more closely, bus 61 emerges as a critical node across all algorithms except the VSA. The SCA places both a 2.2949 MW PV and a 0.3992 Mvar D-STATCOM at this location, while the ASOA installs a 1.5558 MW PV and a 0.4481 Mvar D-STATCOM at bus 61. The NMA places a 1.3118 MW PV and a 0.4279 Mvar D-STATCOM at the same node. This consensus identifies bus 61—located at the far end of the main feeder—as the most electrically disadvantaged location in the network, requiring substantial compensation to maintain voltage within acceptable limits. The VSA, which omits bus 61 entirely from both its PV and D-STATCOM allocations, reports the highest cost among all methods, suggesting that failing to address this critical node compromises economic optimality.

The total installed capacity across algorithms reveals different investment strategies. The NMA installs 3.5364 MW of PV and 0.6475 Mvar of D-STATCOM capacity, while the ASOA installs a few more PVs (3.5878 MW) but a lower D-STATCOM capacity (0.5929 Mvar). The SCA installs 3.5117 MW's worth of PVs and the lowest D-STATCOM capacity (0.5405 Mvar), and the VSA installs the least PVs (3.4878 MW) and an intermediate D-STATCOM capacity (0.5501 Mvar). The NMA's configuration achieves the lowest cost with the highest D-STATCOM capacity relative to the PVs, indicating that its solution places greater emphasis on reactive support. This suggests that, in the 69-bus network, where voltage drop is more severe due to longer feeder lengths, adequate reactive compensation is critical for enabling PV integration and maximizing loss reduction.

In this larger network, the most significant advantage of the NMA is its remarkable computational efficiency. With an average execution time of 1393.39 seconds, the NMA is 13.5% faster than the SCA (1611.16 s), 16.8% faster than the ASOA (1675.35 s), and 17.1% faster than the VSA (1680.10 s). This performance gap widens considerably compared to the 33-bus system, indicating that the NMA's algorithmic efficiency scales more favorably with network complexity. The combination of superior economic performance and a substantially lower computational burden solidifies the NMA's position as the most suitable approach for practical large-scale distribution network planning.

6. Conclusions and future works

This research introduced the NMA for the integrated optimal planning of PVs and D-STATCOMs in medium-voltage distribution networks. The proposed master-slave framework effectively addresses the mixed-integer nonlinear structure of the problem, combining the exploration capabilities of metaheuristics with a gradient-informed search mechanism to navigate the complex solution space. Numerical simulations conducted on standard 33- and 69-bus test systems demonstrated the algorithm's robustness, consistently achieving the lowest total annualized costs—USD 2,290,259.24 and USD 2,395,022.55, respectively—while ensuring full compliance with all operational constraints. These results represent cost reductions of approximately 35.55% compared to the benchmark case, which did not include distributed resources.

A key advantage of the proposed approach is its superior computational efficiency, which becomes more pronounced as network size increases. Compared to other algorithms (VSA, SCA, and ASOA), the NMA reduced processing times by 4.8–6.8% in the 33-bus system and by 13.5–17.1% in the 69-bus feeder. This superior scalability, coupled with the ability to identify well-diversified and technically sound allocation patterns, makes the NMA a particularly suitable tool for real-world distribution system planning, where both solution quality and execution times are critical considerations.

Future research will focus on extending the deterministic framework to incorporate the operational uncertainties arising from renewable generation variability and load fluctuations. A natural progression would involve developing a two-stage stochastic programming model that maintains the convex structure of the power flow equations while enabling robust decision-making under multiple scenarios. This would include systematic sensitivity analyses to evaluate how variations in key economic parameters—such as the discount rate (r_a), the energy cost escalation rate (r_e), and PV capital costs (C_{pv})—affect the optimality of the solutions obtained. Furthermore, comprehensive *what-if* studies under off-design conditions (*e.g.*, cloudy days with reduced solar irradiance or peak load conditions) will be conducted to verify that voltage limits and operational constraints remain satisfied, aiming to demonstrate the practical robustness of the proposed configurations. Additionally, the application of our methodology to meshed network topologies and hybrid AC/DC architectures merits investigations aimed at assessing its performance under more complex grid configurations. Further enhancements could include dynamic operational constraints for battery storage systems and the implementation of real-time model-predictive control strategies to improve the practical adaptability of our proposal.

ACKNOWLEDGEMENTS

The first author would like to thank Oficina de Investigaciones at Universidad Distrital Francisco José de Caldas for supporting the internal research project with code 33787724, titled *Desarrollo de una metodología de gestión eficiente de potencia reactiva en sistemas de distribución de media tensión empleando modelos de programación no lineal*. In addition, the authors acknowledge the assistance of the DeepSeek AI language model in refining the manuscript's language and structure. The tool was used solely for editorial purposes—such as rephrasing, grammar correction, and improving readability—whereas all technical formulations, methodological developments, numerical simulations, and scientific interpretations were conceived and executed by the authors.

Nomenclature

Binary Variables

x_i^{comp}	Binary variable: 1 if the D-STATCOM is installed at bus i, 0 otherwise
x_i^{pv}	Binary variable: 1 if the PV is installed at bus i, 0 otherwise

Parameters

$\beta_{j,l}$	Uniform random number $\in [0, 1]$ for initialization
Δh	Duration of time interval h (h)

ϵ	Numerical tolerance for power flow convergence
Γ	Gradient-like curvature factor
γ	Scaling factor for compensation costs
λ_k	Penalty coefficient for constraint k
$\mathbf{X}^t$	Population matrix at iteration p
$\mathbf{x}_j$	Solution vector for the j-th candidate
$\mathbf{Y}_{dd}$	Admittance submatrix for the demand nodes (S)
$\mathbf{Y}_{dg}$	Coupling admittance submatrix between the demand and slack nodes (S)
$\mathbf{Y}_{gd}$	Transpose of $\mathbf{Y}_{dg}$ (S)
$\mathcal{U}[a, b]$	Continuous uniform distribution on $[a, b]$
$\omega_1, \omega_2, \omega_3$	D-STATCOM cost coefficients
τ	Relative distance ratio between candidate solutions
φ_{ij}	Phase angle of the line admittance between buses i and j (rad)
C_{kWh}	Cost of energy purchased (\$/kWh)
$C_{O\&M}^{pv}$	PV operation and maintenance cost (\$/kWh)
C_{pv}	Unit cost of investment in PV capacity (\$/kW)
$f(\cdot)$	Objective (fitness) function evaluated for a solution candidate
f_a	Annualization factor
f_c	Energy cost escalation factor
$F_f(\cdot)$	Penalized fitness function
$g_k(\mathbf{x})$	k-th inequality constraint (≤ 0)
$G_{i,h}^{pv}$	PV generation factor at bus i during period h (pu)
j	Imaginary unit ($j^2 = -1$)
K	Total number of inequality constraints
n_s	Population size (number of candidate solutions)
n_v	Number of decision variables per candidate
N_y	Planning horizon (years)
N_{comp}^{ava}	Maximum number of D-STATCOM units
N_{pv}^{ava}	Maximum allowable number of PV units
$P^{pv,\max}$	Maximum allowable PV unit size (kW)
$P^{pv,\min}$	Minimum allowable PV unit size (kW)

$P_{i,h}^{d}$	Active power demand at bus i during period h (kW)
$Q^{comp,\max}$	Maximum D-STATCOM capacity (kvar)
$Q^{comp,\min}$	Minimum D-STATCOM capacity (kvar)
$Q_{i,h}^{d}$	Reactive power demand at bus i during period h (kvar)
r_1, r_2	Uniform random numbers $\in [0, 1]$
r_a	Annual discount rate (per unit)
r_e	Annual energy cost escalation rate (per unit)
T	Number of days in a year
t	Current iteration index
$t_{\max}$	Maximum number of iterations
$v^{\max}$	Maximum allowable voltage magnitude (p.u.)
$v^{\min}$	Minimum allowable voltage magnitude (p.u.)
Y_{ij}	Magnitude of the line admittance between buses i and j (S)
Sets	
$\mathcal{H}$	Set of time intervals in the operational horizon
$\mathcal{N}$	Set of network buses (nodes)
$\mathcal{T}$	Set of years in the planning period
Variables	
$\mathbf{S}_{d,h}^{*}$	Net complex power injection at the demand nodes for period h (VA)
$\mathbf{S}_{d,h}^{dg}$	Complex power from conventional distributed generation (VA)
$\mathbf{S}_{d,h}^{load}$	Complex power demand at the load nodes (VA)
$\mathbf{S}_{g,h}$	Complex power supplied by the slack bus (VA)
$\mathbf{S}_{h}^{comp}$	Complex power from D-STATCOMs (reactive only) (VA)
$\mathbf{S}_{h}^{pv}$	Complex power from PVs (active only) (VA)
$\mathbf{V}_{d,h}$	Complex voltage vector at the demand nodes for period h (V)
$\mathbf{V}_{g,h}$	Complex voltage at the slack bus for period h (V)
$\mathbf{x}_{\text{best}}^{t}$	Elite (best) solution at iteration p
$\theta_{i,h}$	Voltage angle at bus i during period h (rad)
$C_{\text{D-STATCOM}}$	Annualized D-STATCOM investment cost ($)
C_{GRID}	Annualized cost of grid energy purchases ($)
$C_{\text{PV}}^{\text{invest}}$	Annualized PV capital investment cost ($)

$C_{\text{PV}}^{\text{O\&M}}$	Annual PV operating and maintenance costs ($)
C_{TOTAL}	Total annualized system cost ($)
$p_{i,h}^{cg}$	Active power from conventional generation at bus i in period h (kW)
$p_{i,h}^{pv}$	Actual PV generation at bus i in period h (kW)
p_{i}^{pv}	Rated PV capacity at bus i (kW)
$q_{i,h}^{cg}$	Reactive power from conventional generation at bus i in period h (kvar)
$q_{i,h}^{comp}$	Dispatched D-STATCOM compensation at bus i during period h (kvar)
q_{i}^{comp}	Rated D-STATCOM capacity at bus i (kvar)
$v_{i,h}$	Voltage magnitude at bus i during period h (p.u.)

REFERENCES

1. Asit Mohanty, A.K. Ramasamy, Renuga Verayiah, Satabdi Bastia, Sarthak Swaroop Dash, Erdem Cuce, T.M. Yunus Khan, and Manzoore Elahi M. Soudagar. Power system resilience and strategies for a sustainable infrastructure: A review. *Alexandria Engineering Journal*, 105:261–279, October 2024.
2. Bilal Khan, Sadam Hussain, Hayat Ullah, Chunyan Lai, Ahmed A. Mohamed, and Ursula Eicker. Low voltage distribution grids optimization with increasing distributed energy generation: A review. *Energy Reports*, 15:108913, June 2026.
3. Steve Sorrell. Reducing energy demand: A review of issues, challenges and approaches. *Renewable and Sustainable Energy Reviews*, 47:74–82, July 2015.
4. Tiku Fidelis Etanya, Pierre Tsafack, and Divine Khan Ngwashi. Grid-connected distributed renewable energy generation systems: Power quality issues, and mitigation techniques – A review. *Energy Reports*, 13:3181–3203, June 2025.
5. Saeed Al-Ali, Abdul Ghani Olabi, and Montaser Mahmoud. A review of solar photovoltaic technologies: developments, challenges, and future perspectives. *Energy Conversion and Management: X*, 27:101057, July 2025.
6. P.A.G.M. Amarasinghe, S.K. Abeygunawardane, and C. Singh. Reliability evaluation of solar integrated power distribution systems using an Evolutionary Swarm Algorithm. *Engineering Applications of Artificial Intelligence*, 149:110464, June 2025.
7. Oscar Danilo Montoya Giraldo, Edwin Rivas-Trujillo, and Luis Fernando Grisales Noreña. Advanced Sech-Tanh Optimization Algorithm for Optimal Sizing and Placement of PV Systems and D-STATCOMs in Distribution Networks. *Statistics, Optimization & Information Computing*, 13(5):1933–1946, January 2025.
8. Oscar Danilo Montoya, Carlos Alberto Ramírez-Vanegas, and Luis Fernando Grisales-Noreña. A Sine-Cosine Algorithm Approach for Optimal PV and D-STATCOM Integration in Distribution Systems. *Statistics, Optimization & Information Computing*, 13(3):1266–1279, November 2024.
9. Adriana Rincón-Miranda, Giselle Viviana Gantiva-Mora, and Oscar Danilo Montoya. Simultaneous integration of d-statcoms and pv sources in distribution networks to reduce annual investment and operating costs. *Computation*, 11(7):145, July 2023.
10. Abere Takele Alemu and Getaneh Mesfin Meseret. Optimal Location and Sizing of Static Var Compensator (SVC) to Improve Voltage Profile in Distribution Network. *Engineering Reports*, 7(10), October 2025.
11. Kanaga Bharathi N, Manoharan Abirami, Devi Vighneshwari, and Manoharan Hariprasath. Techno-economic optimization of hybrid renewable systems for sustainable energy solutions. *Scientific Reports*, 15(1), July 2025.
12. Oscar Danilo Montoya Giraldo, Luis Fernando Grisales Noreña, and Rubén Iván Bolaños. Optimal Placement and Sizing of PV Systems and D-STATCOMs in Medium-Voltage Distribution Networks Using the Atan-Sinc Optimization Algorithm. *Statistics, Optimization & Information Computing*, 14(5):2365–2378, July 2025.
13. Rajiv K. Varma and Ehsan M. Siavashi. Pv-statcom: A new smart inverter for voltage control in distribution systems. *IEEE Transactions on Sustainable Energy*, 9(4):1681–1691, October 2018.
14. Mezigebu Getinet Yenealem. Optimum Allocation of Microgrid and D-STATCOM in Radial Distribution System for Voltage Profile Enhancement Using Particle Swarm Optimization. *International Journal of Photoenergy*, 2024(1), January 2024.
15. Saeed Gholizadeh, Masood Danesh, and Changiz Gheyratmand. A new Newton metaheuristic algorithm for discrete performance-based design optimization of steel moment frames. *Computers & Structures*, 234:106250, July 2020.
16. Oscar Danilo Montoya, Walter Gil-González, and Luis Fernando Grisales-Noreña. Optimal planning of photovoltaic and distribution static compensators in medium-voltage networks via the gndo approach. *Results in Engineering*, 23:102764, September 2024.
17. Oscar Danilo Montoya and Walter Gil-González. On the numerical analysis based on successive approximations for power flow problems in ac distribution systems. *Electric Power Systems Research*, 187:106454, October 2020.
18. Oscar Danilo Montoya, Walter Gil-González, Rubén Iván Bolaños, Diego Fernando Muñoz-Torres, Jesús C. Hernández, and Luis Fernando Grisales-Noreña. Effective power coordination of besus in distribution grids via the sine-cosine algorithm. In *2024 IEEE Green Technologies Conference (GreenTech)*. IEEE, April 2024.

19. Daniel Julián Nivia Torres, Guillermo Alejandro Salazar Alarcón, and Oscar Danilo Montoya Giraldo. Optimal Selection of Conductors in Three-Phase Distribution Networks using the Newton Metaheuristic Algorithm (In Spanish). *Ingeniería*, 27(3):e19303, August 2022.
20. Luis Fernando Grisales-Noreña, Daniel Sanin-Villa, and Oscar Danilo Montoya. Optimal integration of PV generators and D-STATCOMs into the electrical distribution system to reduce the annual investment and operational cost: A multiverse optimization algorithm and matrix power flow approach. *e-Prime - Advances in Electrical Engineering, Electronics and Energy*, 9:100747, September 2024.